THE JOURNAL OF PHYSICAL CHEMISTRY B

ARTICLE

pubs.acs.org/JPCB

Osmium Bipyridine-Containing Redox Polymers Based on Cellulose and Their Reversible Redox Activity

Hongliang Kang,[†] Ruigang Liu,[*,†] Huafeng Sun,[§] Jieming Zhen,[§] Qinmei Li,[†,∥] and Yong Huang[*,†,‡]

[†]Laboratory of Polymer Physics and Chemistry, Beijing National Laboratory of Molecular Sciences, Institute of Chemistry, and [‡]Technical Institute of Physics and Chemistry, Chinese Academy of Sciences, Beijing 100190, China

[§]Department of Chemistry, School of Science, Beijing Jiaotong University, Beijing 100044, China

[∥]Graduate University, Chinese Academy of Sciences, Beijing 100039, China

Supporting Information

ABSTRACT: Thermo-, pH-, and electrochemical-sensitive cellulose graft copolymers, hydroxypropyl cellulose-*g*-poly(4-vinylpyridine)-Os(bipyridine) (HPC-*g*-P4VP-Os(bpy)), were synthesized and characterized. The electrochemical properties of the resulting material were investigated via cyclic voltammetry by coating the graft copolymers on the platinized carbon electrode. The results indicated that the electrochemical properties of the graft copolymer modified electrode were responsive to the pH values of the electrolyte solution. The reversible transformation between the active and inactive state originated from the changes in the architecture of the HPC-*g*-P4VP-Os(bpy) graft copolymer at different pH values. At high pH (e.g., above the pK_a of P4VP), the chains of P4VP collapsed, and the electrochemical activity of the electrode was reduced. With immobilization of glucose oxidase (GOx) on the graft copolymer decorated electrode, a biosensor for glucose detection was prepared. The current of the biosensor depended on the glucose concentration in the detected solution and increased with the successive addition of glucose.

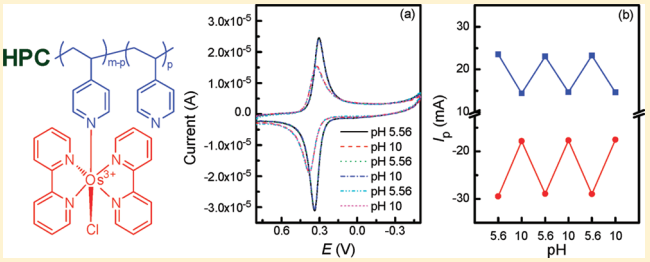

INTRODUCTION

Stimuli-responsive polymers have attracted increasing attention in past decades. The responses of such polymers to the environmental stimuli such as temperature,[1−4] pH,[5,6] ionic strength,[7−9] light,[10,11] biological conditions,[12] or mechanical stress[13,14] offer them potential applications in many fields including oil recovery,[15,16] water decontamination,[17−19] analytical chemistry,[20,21] purification techniques,[22] antibacterial coatings,[23] and biomedicine.[24,25] More recently, copolymers with well-defined architecture and multi stimuli-responsive properties were developed on the basis of controlled/living polymerizations.

In the last 10 years, cellulose graft copolymers with well-defined architecture were synthesized for the purpose of combining the properties of both the cellulose backbone and the side chains, which could offer cellulose graft copolymer new applications in many fields. In our previous works, series stimuli-responsive cellulose graft copolymers have been synthesized and investigated extensively.[26−34] The stimuli-responsive property of the cellulose graft copolymers can be tailored either by the cellulose backbone (e.g., HPC is thermal sensitive in aqueous solution) or by the chemical structure of the side chains. The cellulose graft copolymers can self-assemble into single-[26−28,35] or multi-stimuli[32−34,36] responsive micelles in the selected solvents depending on the components of the graft copolymers. Cellulose is a kind of polymer with renewable, inexpensive, and biodegradable properties. Its stimuli-responsive micelles have potential applications as carriers for drug and gene delivery and in controlled release.[26,35,37] The cellulose graft copolymers generally have the reversible thermal or/and pH stimuli-responsive properties in the literature. However, few works on the cellulose graft copolymers with redox stimuli responsive property have been reported.[29]

Redox polymers are usually used in the chemically modified electrodes, which has attracted attention due to their variable properties, particularly on the applications for bioelectroanalysis and biosensors. The redox polymers coated onto electrode surfaces can mediate charge transfer between the electrode and the target solution species. Generally, two types of redox polymers have been reported in the literature depending on the location of the redox groups. One is polymers with redox groups on the backbone, such as poly(vinyl hydroquinone)s.[38] The other is those polymers contain pendent redox groups or graft chains with redox groups, such as osmium complex or ferrocence.[39,40] Osmium complex of poly(4-vinylpyridine)[41] or poly(*N*-vinylpyrrole)[42] is the typical redox polymer of the later case and has been widely studied due to their altering the formal potential with different structures of ligands. These osmium complex polymers have been applied as the mediators in the biosensors for the detection of dopamine,[43] ascorbic acid,[44] lactate,[45] glucose,[46] H_2O_2,[47] etc.

Received: August 30, 2011
Revised: December 6, 2011
Published: December 07, 2011

In those enzyme electrodes, the structure of the polymer is one of the key factors that affects the performance of polymer-coated electrodes by the effect on the electron transfer rate, surface coverage (concentration) of redox active centers, charge transport and propagation, as well as diffusion and permeation of soluble species through the polymer.[48] Specially, for the purpose of good contact with water-soluble enzymes, the redox polymers are expected to be hydrophilic, such as poly(4-vinylpyridine) osmium complex usually modified by amine to enhance its solubility in water.[49]

In this Article, hydroxypropylcellulose-*g*-poly(4-vinylpyridine)-Os(bipyridine) (HPC-*g*-P4VP-Os(bpy)) graft copolymers were synthesized and characterized. The water-soluble HPC backbone offered the solubility or swelling of the graft copolymers in water. The redox activity of the HPC-*g*-P4VP-Os(bpy) was investigated at different pH values. By immobilization of the glucose oxidase (GOx) on the graft copolymers-coated electrode, a sensor was fabricated for the detection of glucose.

EXPERIMENTS

Materials. 4-Vinylpyridine (4VP) (95%, Acros) was distilled from calcium hydride under reduced pressure before use. Hydroxypropyl cellulose (HPC) (M_n = 10 000 g/mol, M_w = 80 000 g/mol, Aldrich) was dried for 48 h under a vacuum at 50 °C before use. poly(vinyl pyridine) (P4VP) (M_w = 60 000 g/mol, Aldrich), ammonium ceric nitrate (CAN) (A.R. grade, Aladdin), K_2OsCl_6 (99%, Alfa Aesar), and 2,2′-bipyridine (98%, Aldrich) were used as received. Other chemicals (A.R. grade) were supplied by local chemical suppliers and used as received. The water was Milli-Q water. Dialyser had the cutoff molecular weight of 14 kDa. Glucose oxidase (>100 U/mg, Aladdin) was used as received.

Synthesis of Hydroxypropylcellulose-*g*-poly(4-vinylpyridine) (HPC-*g*-P4VP). Hydroxypropylcellulose-*g*-poly(4-vinylpyridine) (HPC-*g*-P4VP) copolymers were synthesized by free radical graft copolymerization initiated by CAN. In detail, HPC was dissolved in water under continuous stirring and bubbled with N_2 to remove oxygen in the solution. The solution was then transferred to an oil bath settled at 35 °C, and nitric acid was added until the pH value of the solution was 1.0. Next, degassed 4VP was added and dissolved for 15 min, after which the degassed initiator of CAN aqueous solution was added. The reaction vessel was then sealed, and the reaction was stopped by adding hydroquinone at a desired period of reaction time. The reaction mixture was dialyzed against water to remove unreacted monomers and its low molecular weight homopolymers and other impurities. The graft copolymers were obtained by freeze-drying after dialysis in water for 5 days.

Synthesis of HPC-*g*-P4VP-Os(bpy) Complex. HPC-*g*-P4VP-Os(bpy) complex was synthesized by the reaction of HPC-*g*-P4VP graft copolymers with $Os(bpy)_2Cl_2$. $Os(bpy)_2Cl_2$ was synthesized as follows. K_2OsCl_6 and 2,2′-bipyridine (1:2, mole ratio) were dissolved in 5 mL of DMF and refluxed at 140 °C in an oil bath for 3 h. The reaction mixture was cooled to room temperature, and KCl crystals were formed in the reaction mixture. KCl crystals were filtered, and the left solution was diluted by adding 3 mL of ethanol and precipitated in ether. The crude $Os(bpy)_2Cl_3 \cdot 2H_2O$ was collected by centrifugation and dried in air overnight, and was then dissolved in the methanol/DMF/H_2O (volume ratio of 1:2:20) mixture solvent. The $Na_2S_2O_4$ solution was added dropwise to precipitate $Os(bpy)_2Cl_2$. The purified $Os(bpy)_2Cl_2$ was collected by centrifugation and dried in a vacuum. Product yield: 68.3%.

$Os(bpy)_2Cl_2$ and HPC-*g*-P4VP (1/1, w/w) were dissolved in glycol and refluxed for 24 h to obtain HPC-*g*-P4VP-Os(bpy) complex. The reaction mixture was dialyzed against deionized water for 3 days with refreshing the outer deionized water twice a day and freeze-dried to obtain the solid product. Product yield: 48.4%.

Modification of Electrode. Before modification, the bare platinized carbon working electrode was carefully polished with alumina powder (0.1 and 0.05 μm, respectively) on chamois leather and then thoroughly cleaned ultrasonically in ethanol and distilled water. HPC-*g*-P4VP-Os(bpy) was first dissolved in deionic water (1.95 g/L). Next, 5 μL of the solution was coated on the platinized carbon electrode (Φ 3 mm) and left for 1 h to dry. For preparing enzyme and HPC-*g*-P4VP-Os(bpy) copolymer-coated electrode, HPC-*g*-P4VP-Os(bpy) copolymer (10 g/L) and glucose oxidase (15 g/L) aqueous solution were mixed in a volume ratio of 1:1. 5 μL of this solution was coated on the platinized carbon electrode and left for 1 h to dry.

Characterizations. ^{1}H NMR measurements were carried out with a Bruker DMX 400 NMR instrument using dimethyl sulfoxide-d_6 as the solvent. FT-IR spectra were recorded on a Bruker-Equinox 55 FT-TR spectrometer by KBr method. The molecular weight and the molecular weight distribution of HPC and the graft copolymers were measured by gel permeation chromatography (GPC) (Waters 515), on a system equipped with a Waters 515 pump, three columns, and a 2410 differential refractometer detector. DMF was used as the eluant at the flow rate of 0.5 mL/min. Monodisperse polystyrene was used as the standard to generate the calibration curve. Elemental analysis (CHN) was performed on a Flash EA 1112 elemental analyzer. Os content in graft copolymer was determined by inductively coupled plasma (ICP) atomic emission spectroscopy (Varian 710-ES, U.S.).

Dynamic light scattering (DLS) experiments were carried out on a commercial spectrometer (ALV/SP-150) equipped with an ALV-5000 multi-τ digital time correlator and a solid-state laser (ADLS DPY 425II, output power about 400 MW at λ = 632.8 nm) as the light source. All copolymer solutions were 1 mg/mL and filtered through the Milipore Millex-FH nylon filter (0.45 μm) before measurements. The hydrodynamic radius (R_h) was obtained by fitting the correlation function with the CONTIN program. The samples were equilibrated for 30 min at the desired temperature that was controlled by a thermostatic bath. All DLS experiments were carried out at the scattering angle of 90°.

The transmittance of the copolymer solution was determined at the fixed wavelength of 500 nm on a Shimadzu 1601PC UV—vis spectrophotometer. The concentration of the polymer was kept at 1 mg/mL in aqueous solution.

Electrochemical experiments were carried out on a CHI660D electrochemical workstation (CH instruments, Chenhua Instruments Corp., Shanghai, China). The three-electrode system consisted of a platinized carbon electrode as working electrode, a Pt wire as secondary electrode, and Ag|AgCl as the reference electrode. Cyclic voltammeters were carried in a 0.1 M phosphate buffer solution.

RESULTS AND DISCUSSION

Synthesis of HPC-*g*-P4VP-Os(bpy). The synthesis route of HPC-*g*-P4VP-Os(bpy) is shown in Scheme 1. First, HPC-*g*-P4VP is synthesized by using free radical polymerization with Ce^{4+} as the initiator in aqueous solution. Because HPC is a

dx.doi.org/10.1021/jp2083488 |J. Phys. Chem. B 2012, 116, 55–62

Scheme 1. Preparation Process of HPC-*g*-P4VP-Os(bpy)

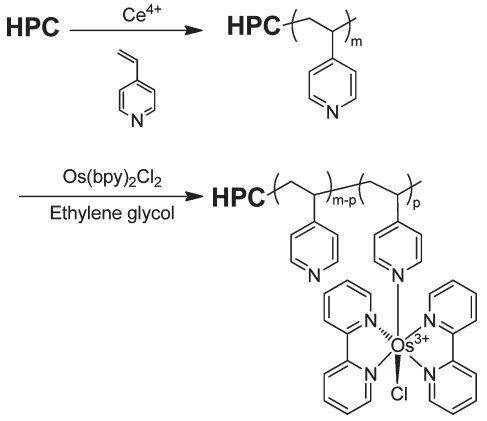

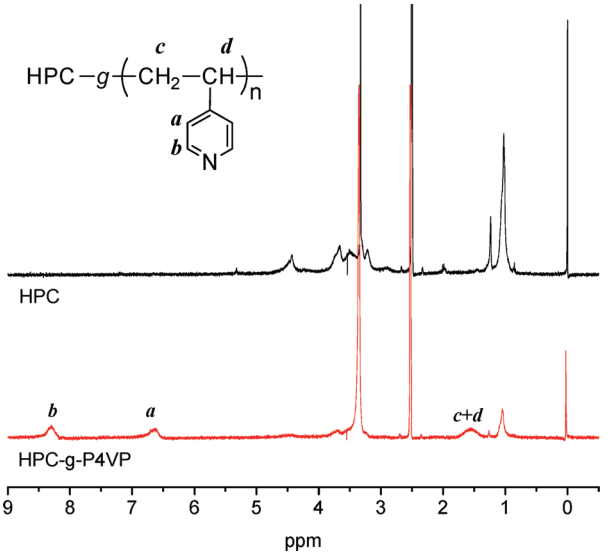

Figure 1. ^{1}H NMR spectra of HPC-*g*-P4VP and HPC in DMSO-d_6 solvent.

thermal-sensitive polymer with the LCST of 45 °C, the graft copolymerization is carried out at 35 °C to keep the good solubility of HPC in aqueous solution. The content of the P4VP in the HPC-*g*-P4VP graft copolymers was adjusted by varying the concentration of the initiator CAN and monomer 4VP in the reaction system as well as the reaction time (details are available in the Supporting Information). The graft copolymers are purified by dialysis against water to remove the free P4VP and unreacted monomers. Next, the HPC-*g*-P4VP-Os(bpy) is synthesized by complexation between the nitrogen in the pyridine ring of the P4VP side chains and osmium-bipyridine.

Figure 1 shows the ^{1}H NMR spectra of HPC and HPC-*g*-P4VP. The multiple peaks around δ = 3.0−5.0 ppm and the single peak at δ = 1.1 ppm are attributed to the protons of glucose rings and methyl protons of HPC, respectively. The new characteristic chemical shifts at about 8.3, 6.6, and 1.5 ppm correspond to the protons of P4VP. On the FT-IR spectra (Figure 2), the bands at 3439 and 1083 cm^{-1} are attributed to the stretching of −OH and C−O−C in glucose rings of HPC. The prominent additional bands at 1597 and 1556 cm^{-1} are due to the stretching

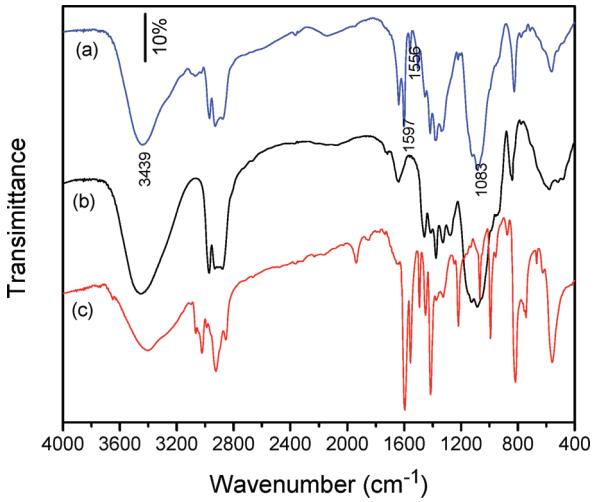

Figure 2. FTIR spectra of (a) HPC-*g*-P4VP, (b) HPC, and (c) P4VP.

of pyridine groups of P4VP. These results confirm the success of the synthesis of HPC-*g*-P4VP.

The success of the complexing of −Os(bpy)$_2$ onto the HPC-*g*-P4VP graft copolymers was characterized by UV−vis absorption spectra. The content of Os in the complex graft copolymers was determined by inductively coupled plasma (ICP) atomic emission spectroscopy, and the results are listed in Table 1. Figure 3 shows the UV−vis absorption spectra of HPC-*g*-P4VP-Os(bpy), HPC-*g*-P4VP, and Os(bpy)$_2$Cl$_2$. They exhibit the characteristic metal-to-ligand charge-transfer (MLCT) bands in the visible region.[50] After $[Os(bpy)_2]^{2+}$ complexes with the pyridine groups of P4VP side chains of the cellulose graft copolymer, the bands move to lower wavenumber. Two kinds of HPC-*g*-P4VP copolymers with different branch length were used to function to osmium. As shown in Table 1, samples A1 and A2 have a similar content of P4VP (6.76 repeat units of 4VP for every glucose ring in cellulose) and different contents of Os. The different amounts of the Os complex bound to the branch chains of P4VP were obtained by changing the mole ratio of HPC-*g*-P4VP and Os(bpy)$_2$Cl$_2$. Figure 4 shows the hydrodynamic radius (R_h) distribution of HPC-*g*-P4VP-Os(bpy) and HPC-*g*-P4VP in aqueous solution. The result indicates that the $\langle R_h \rangle$ of the HPC-*g*-P4VP graft copolymer is about 50 nm. After HPC-*g*-P4VP copolymer is functionalized with −Os(bpy)$_2$ redox units, the $\langle R_h \rangle$ of HPC-*g*-P4VP-Os(bpy) is about 92 nm. This is because the pendant redox unit −Os(bpy)$_2$ is hydrophobic, which may cause the association of the graft copolymers.

Temperature and pH Response. HPC is a thermo-sensitive polymer with the LCST at around 45 °C. It can form metastable nanoparticle aggregates in aqueous solution via chain association at only a couple of degrees higher than LCST.[51] Figure 5 represents the transmittance as a function of temperature of HPC, HPC-*g*-P4VP, and HPC-*g*-P4VP-Os(bpy) in water. The results show that for the graft copolymer HPC-*g*-P4VP$_{6.76}$, which has high content of P4VP, the transmittance of the solution is independent of the temperature. This is because the properties of the HPC backbones have been changed by the high graft density and P4VP content. For the graft copolymer with relatively lower P4VP content, HPC-*g*-P4VP$_{2.07}$, the transmittance of the solution starts to decrease at about 50 °C, and the solution becomes opaque during the process. The reason is that when the temperature of the solution is above its LCST, the HPC backbones

dx.doi.org/10.1021/jp2083488 |*J. Phys. Chem. B* 2012, 116, 55–62

become hydrophobic and collapse to form a core that stabilized with hydrophilic P4VP side chains at the surface of the HPC aggregation. The opaque solution is stable and turns transparent again when the temperature of the solution decreases to a temperature lower than its cloud point, for example, room temperature. From the curve of the transmittance versus the temperature, the cloud point of the HPC-*g*-P4VP$_{2.07}$ can be estimated at about 55 °C, which is higher than that of HPC. The increase of cloud point of the graft copolymer may be due to the higher hydrophilic content in the graft copolymer. The thermal sensitivity of the HPC-*g*-P4VP graft copolymers has been discussed in detail in previous work, which is because the HPC backbone collapses to form the core of the micelles that stabilized with P4VP in the shell of the micelles.[32] The graft copolymer HPC-*g*-P4VP$_{2.07}$ functionalized with $-$Os(bpy)$_2$ redox units also shows thermal sensitivity with a cloud point at about 54 °C, as that indicated the transmittance as a function of temperature (Figure 5). Above the LCST, the graft copolymer can assemble into micelles with a diameter around 100 nm (Figure 6).

P4VP is a weak polyelectrolyte (p$K_a \approx 5$) and becomes hydrophobic and precipitates from aqueous solution at pH > 5 due to deprotonation of nitrogen atoms in the pyridine rings.[52,53] In case of HPC-*g*-P4VP graft copolymers, the hydrophilic HPC backbone is expected to stabilize the P4VP side chains to aggregate, preventing precipitation from the aqueous solution at pH > 5. HPC-*g*-P4VP$_{6.76}$-Os(bpy) also shows a pH-sensitive property. Figure 7 is the transmittance of the HPC-*g*-P4VP$_{6.76}$-Os(bpy) solution in water at different pH values. It can be seen that the transmittance of solution decreases constantly with the increase in the pH values until the graft copolymer precipitates at about pH 13. It cannot assemble into stable micelles after increasing the pH values, forming aggregations. The result is different from previous work, in which the HPC-g-P4VP graft copolymers synthesized by ATRP can form stable micelles at higher pH values.[32] This may be attributed to that the pK_a of the HPC-*g*-P4VP graft copolymers depends on the architecture (block or graft) and the length of P4VP chains.[54] The deprotonation of pyridine groups in HPC-*g*-P4VP$_{6.76}$-Os(bpy) with the pH value increasing makes the macromolecules more hydrophobic and aggregate.

Electrochemical Response. The electrochemical properties of the redox-functionalized cellulose graft copolymer modified electrode were studied by cyclic voltammetry. The results indicate that samples A1 and A2 have electrochemical responsive properties. However, sample B1 does not show electrochemical responsive properties. Figure 8a shows cyclic voltammograms of the electrode coated with sample A1 at different potential scan rates at pH 7.4. The results indicate that the cyclic voltammograms are the reversible electrochemical process at low potential scan rates. The standard potential $E^\circ = 0.333$ V, with peak-to-peak separation $\Delta E_p = 59/n$ mV ($n = 1$, the number of electrons in a single electro transfer acts characteristic of the Os-complex electrochemistry[55]) at potential scan rate $v = 100$ mV/s. Moreover, the peaks on the cyclic voltammograms are stable for many potential cycles and the washing of the electrode. However, I_p is proportional to the square root of the potential scan rate (Figure 8b), different from the theoretical prediction that I_p

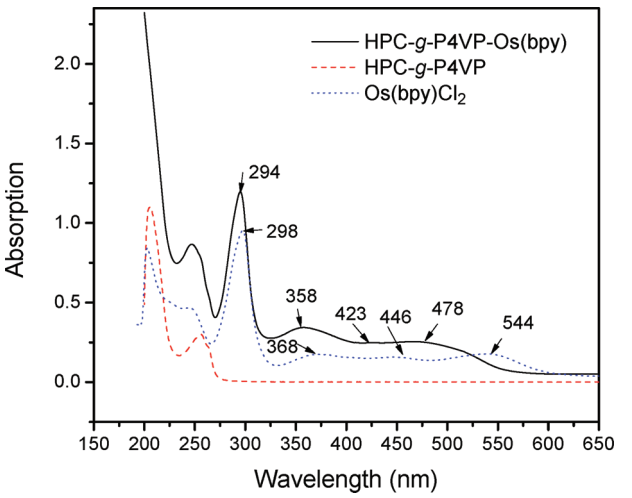

Figure 3. UV−vis absorption spectra of HPC-*g*-P4VP-Os(bpy), HPC-*g*-P4VP, and Os(bpy)$_2$Cl$_2$ in methanol.

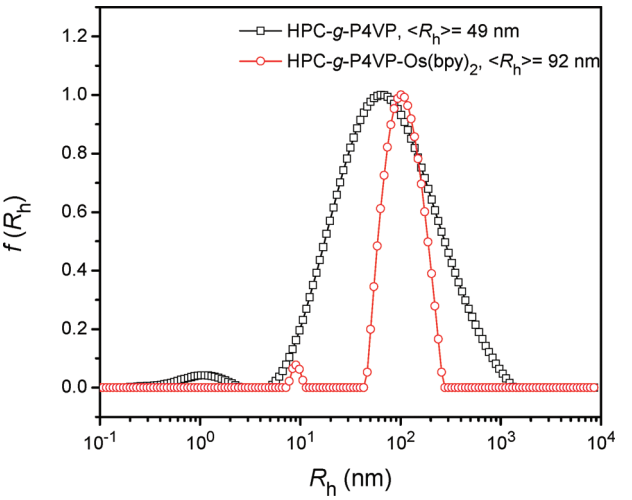

Figure 4. Size distributions of HPC-*g*-P4VP and HPC-*g*-P4VP-Os(bpy) in aqueous solution at 25 °C. The concentration is 1 mg/mL.

Table 1. Summary of Characteristic Data of the Graft Copolymers HPC-*g*-P4VP-Os(bpy)

			repeat unit of P4VP			
HPC-*g*-P4VP-Os(bpy)	M_n (g/mol)[a]	PDI	EA[b]	NMR[c]	content of Os (μmol/mg)[d]	4VP/Os (mole ratio)
A1	7.45×10^5	1.30	3.24	6.76	0.54[e]	11.85
A2	7.45×10^5	1.30	3.24	6.76	1.40[f]	4.55
B1	9.47×10^4	3.34	2.52	2.07	0.37	1.02

[a] GPC analysis of HPC-*g*-P4VP. [b] The calculated results from CHN elemental analysis, representing the repeat units of branch P4VP as compared to every glucose ring. [c] The calculated results from ^{1}H NMR analysis, representing the repeat units of branch P4VP as compared to every glucose ring. [d] The content of Os element by ICP characterized. [e] The reaction ratio of HPC-*g*-P4VP and Os(bpy)$_2$Cl$_2$ is 2/1 (w/w). [f] The reaction ratio of HPC-*g*-P4VP and Os(bpy)$_2$Cl$_2$ is 1/1 (w/w).

dx.doi.org/10.1021/jp2083488 |J. Phys. Chem. B 2012, 116, 55–62

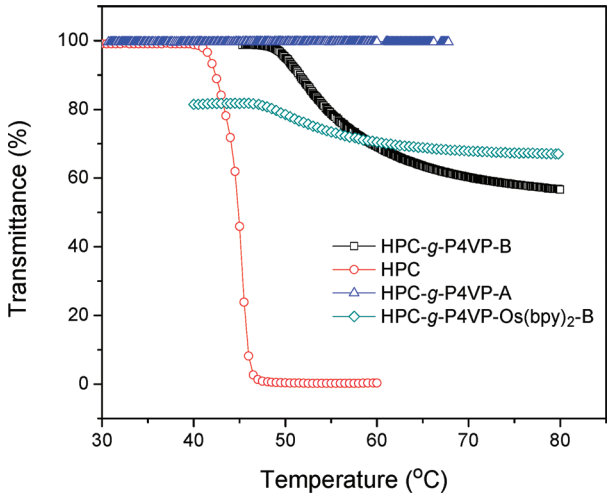

Figure 5. The transmittance against temperature curves for HPC-*g*-P4VP-Os(bpy), HPC-*g*-P4VP copolymers, and HPC.

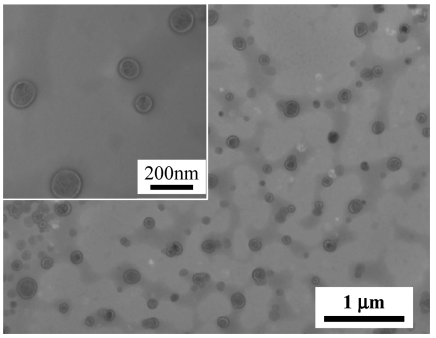

Figure 6. TEM images of micelles of HPC-*g*-P4VP$_{2.07}$-Os(bpy).

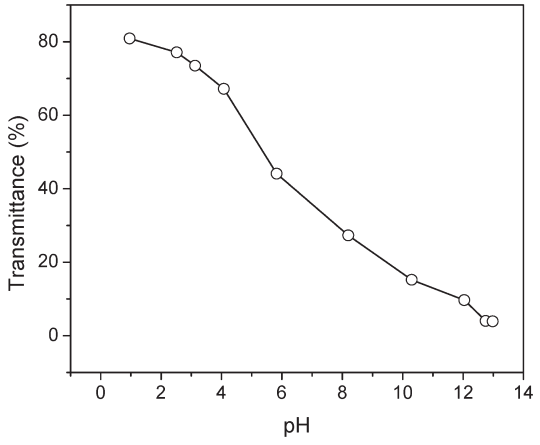

Figure 7. The transmittance against pH curves for HPC-*g*-P4VP$_{6.76}$-Os(bpy).

linearly increases with the elevated potential scan rate for the surface-confined electrochemical process. Such relationship suggests the quasi-diffusional translocation of the redox units bound to the flexible polymer chains on the electrode surface. This phenomenon has also been observed for ferrocene groups linked to the flexible polymer[56,57] or osmium

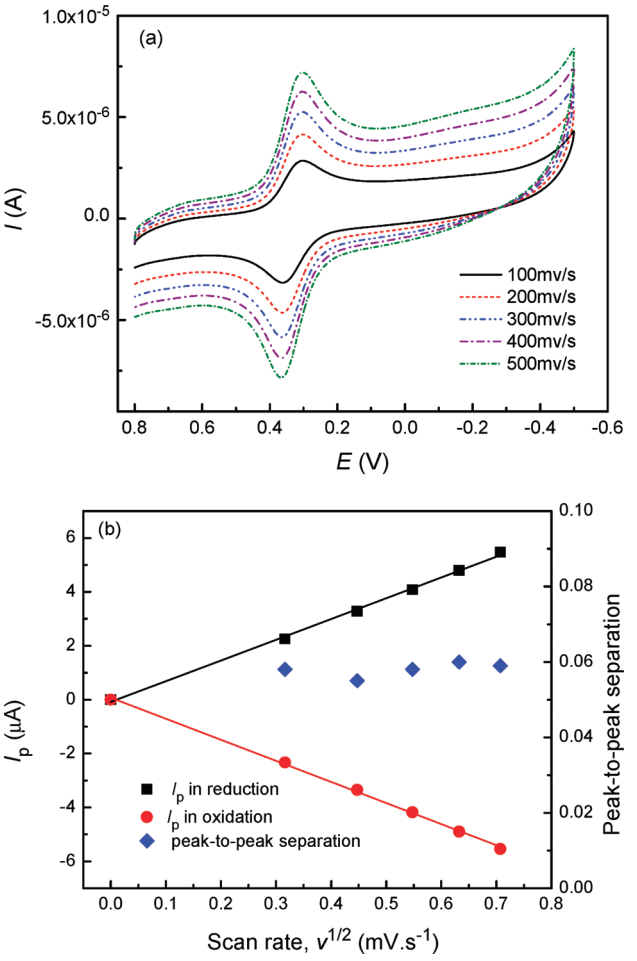

Figure 8. (a) Cyclic voltammograms of the HPC-*g*-P4VP-Os(bpy) modified electrode obtained upon application of different potential scan rates;. (b) The peak current and peak-to-peak separation dependence on the square-root of the potential scan rate. The measurements were performed in 0.1 M phosphate buffer, pH 7.4.

complex with P4VP bound to an electrode.[58] The surface coverage of the electrode with the redox species, $\Gamma = 2.2 \times 10^{-10}$ mol/cm^2 ($n = 1$), by integrating the peak on the cyclic voltammogram was recorded at a low scan rate, $\nu = 100$ mV/s.

The redox property of the graft copolymer HPC-*g*-P4VP-Os(bpy) (sample A1) is also sensitive to pH. Figure 9a shows the cyclic voltammograms of the HPC-*g*-P4VP-Os(bpy) modified electrode with the background solution at different pH values. The cyclic voltammograms indicate that the peak drops at pH 7.0 and becomes weaker with the further increase in pH value until it almost disappears at pH 14.0 (Figure 9b). The $-$Os(bpy)$_2$ pendant redox groups are subjected to the reduction$-$oxidation process without the participation of protons in the reaction, which suggests that the pH value has not affected the redox potential theoretically. It should be noted that the mole ratio of P4VP to Os is 11.85, which means that large amounts of the pyridine ring left without ligand with Os in the HPC-*g*-P4VP-Os(bpy) copolymer. Therefore, the dependence of the redox properties of the HPC-*g*-P4VP-Os(bpy) copolymer on pH is attributed to the deprotonations of the pyridine groups, which leads to the collapse of the graft polymer at higher pH values. As a result, the graft copolymer loses the quasi-diffusion flexibility, and the electrochemical

dx.doi.org/10.1021/jp2083488 |*J. Phys. Chem. B* 2012, 116, 55–62

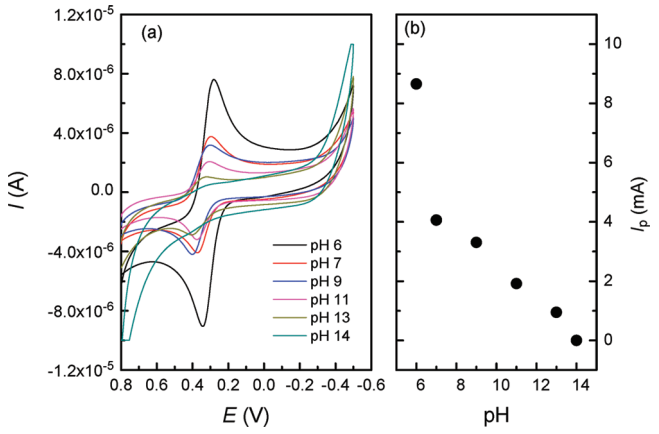

Figure 9. (a) Cyclic voltammograms of the HPC-*g*-P4VP-Os(bpy) modified electrode at different pH values of the background solution. (b) Peak current dependence on the pH value of the background solution. The measurements were performed in 0.1 M phosphate buffer with the potential scan rate, 100 mV/s.

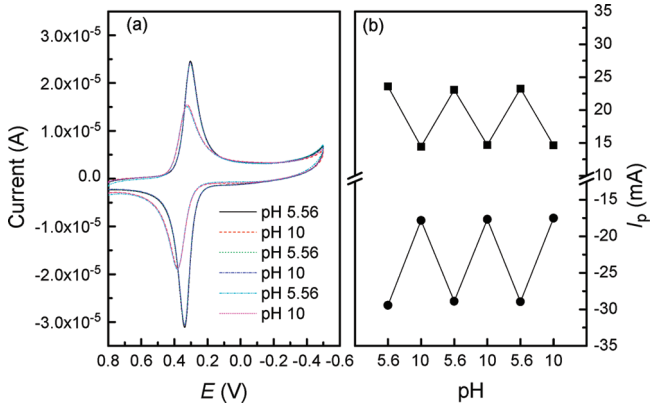

Figure 10. (a) Cyclic voltammograms of the HPC-*g*-P4VP-Os(bpy) modified electrode obtained upon stepwise measurements performed in pH 5.56 and pH 10 solution. (b) Reversible switching of the HPC-*g*-P4VP-Os(bpy) modified electrode activity. The measurements were performed in 0.1 M phosphate buffer with the potential scan rate, 100 mV/s.

activity of the redox groups is reduced. It has been reported that the electrode modified with P4VP-Os-complex redox units shows pH dependence property, and the redox peak disappears on the cyclic voltammogram curve at pH > 6. Specifically, our system can extend to high pH values, such as 11 and 13, at which the cyclic voltammograms of the HPC-*g*-P4VP-Os(bpy) modified electrode can still be measured (Figure 9). This is due to the specific architecture of the HPC-*g*-P4VP graft copolymers. With the increase in the pH value even above the pK_a of P4VP, the HPC backbone is still hydrophilic, which provides the channels for the electrochemical reaction. Our system extends the applications of the P4VP-based redox system.

The above-mentioned pH dependence of the redox property of HPC-*g*-P4VP-Os(bpy) graft copolymers is reversible. Figure 10 shows the electrochemical experiments performed in the solution at pH values of 5.6 and 10 at intervals. The cyclic voltammograms of the HPC-*g*-P4VP-Os(bpy) modified electrode show switchable property and are reproducible for several circles.

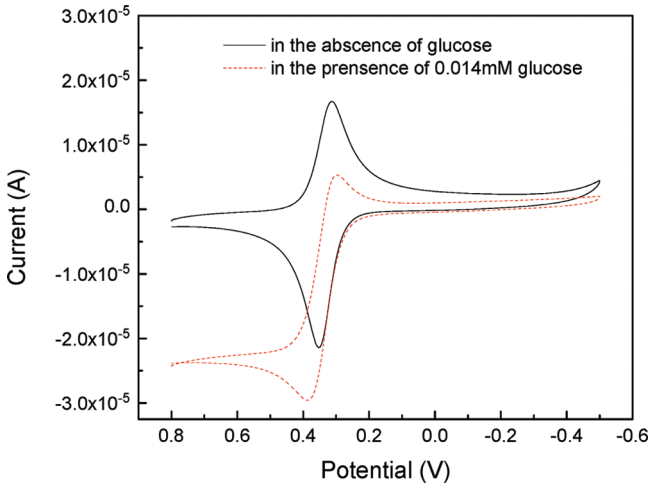

Figure 11. Cyclic voltammograms corresponding to the oxidation of glucose catalyzed by glucose oxidase (GOX), 0.014 mM. The measurements were performed in 0.1 M phosphate buffer (pH 7.0) with the potential scan rate, 50 mV/s.

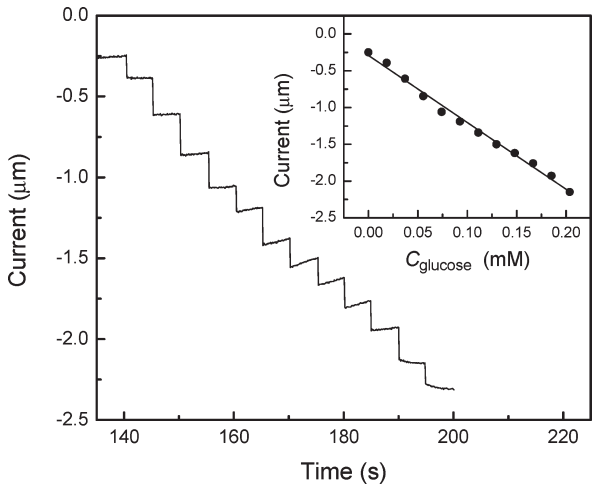

Figure 12. Amperometric response of the GOX/HPC-*g*-P4VP-Os(bpy) biosensor to different concentrations of glucose in PBS (0.1 M, pH 7.0) at an applied potential of 0.4 V. Inset: Calibrated curve of the biosensor with successive addition of glucose.

At low pH (e.g., 5.6), the electrochemical activity of the HPC-*g*-P4VP-Os(bpy) modified electrode is better than that at higher pH (e.g., 10), which is due to that the P4VP side chains collapse and are "frozen" and the electrochemical activity of the electrode is reduced as a result. However, the hydrophiphlic property of the backbone still keeps the electrochemical process.

Application for Glucose Detection. Figure 11 shows the cyclic voltammograms of HPC-*g*-P4VP-Os(bpy) modified electrode in the solutions with and without glucose. The oxidation of glucose is catalyzed by glucose oxidase (GOx). It is shown that the anodic electrocatalytic current corresponding to the oxidation of glucose has been biocatalyzed by GOx and mediated by HPC-*g*-P4VP-Os(bpy) graft copolymer. Figure 12 shows the amperometric response of the GOX/HPC-*g*-P4VP-Os(bpy) biosensor to different concentrations of glucose in PBS (0.1 M, pH 7.0) at an applied potential of 0.4 V. The results indicate that the biosensor

dx.doi.org/10.1021/jp2083488 |*J. Phys. Chem. B* 2012, 116, 55–62

is sensitive to the concentration of glucose and the current obviously increases with the increasing concentration of the glucose. The corresponding calibration curve of the biosensor is shown in the inset of Figure 12. The results show that the current of the GOX/HPC-*g*-P4VP-Os(bpy) modified electrode is linear with glucose concentration with a limit of detection of 0.2 mM. The above results confirm that HPC-*g*-P4VP-Os(bpy) graft copolymer can be used as a matrix that provides a good environment for enzyme activity to enhance the sensitivity of the modified electrode for glucose detection.

CONCLUSION

Cellulose graft copolymers hydroxypropylcellulose-*g*-poly(4-vinylpyridine)-Os(bipyridine) are synthesized through two steps of hydroxypropylcellulose grafted with poly(4-vinylpyridine) by free radical polymerization and then poly(4-vinylpyridine) functionalized with Os-complex redox units. The graft copolymers have temperature, pH, and electrochemical response properties. The electrochemical property of the resulting material deposited as films onto platinized carbon electrode is mainly investigated by cyclic voltammetry. It is found that the electrochemical property of the cellulose graft copolymer-coated electrode is responsive to the pH value of the electrolyte solution. The active and inactive states of the graft copolymer-coated electrodes are reversible, which is attributed to the variation of quasi-diffusion translocation of the P4VP chains due to the protonation and deprotonation of pyridine groups and the swelling and shrinking of the graft copolymer at different pH values. Further immobilization of the glucose oxidase (GOx) on the cellulose graft copolymer electrode can be used as glucose detection sensor. The glucose sensor shows the increase in the current with the increase in the glucose concentration in the media.

ASSOCIATED CONTENT

Supporting Information. Details of the experimental parameters and their effect on the content of the graft P4VP chains of the HPC-*g*-P4VP graft copolymer. This material is available free of charge via the Internet at http://pubs.acs.org.

AUTHOR INFORMATION

Corresponding Author

*Tel.: +8610-82618573. Fax: +8610-62554670. E-mail: rgliu@iccas.ac.cn (R.L.); yhuang@iccas.ac.cn (Y.H.).

ACKNOWLEDGMENT

The financial support of the National Natural Science Foundation of China (Grant nos. 50821062, 20974114, 21174156) is greatly appreciated. We also wish to thank Ping Yu for electrochemical analysis.

REFERENCES

(1) Kostiainen, M. A.; Pietsch, C.; Hoogenboom, R.; Nolte, R. J. M.; Cornelissen, J. *Adv. Funct. Mater.* **2011**, *21*, 2012–2019.
(2) Chang, B. S.; Sha, X. Y.; Guo, J.; Jiao, Y. F.; Wang, C. C.; Yang, W. L. *J. Mater. Chem.* **2011**, *21*, 9239–9247.
(3) Lu, Y.; Ballauff, M. *Prog. Polym. Sci.* **2011**, *36*, 767–792.
(4) Lutz, J. F. *Adv. Mater.* **2011**, *23*, 2237–2243.
(5) El-Khouri, R. J.; Bricarello, D. A.; Watkins, E. B.; Kim, C. Y.; Miller, C. E.; Patten, T. E.; Parikh, A. N.; Kuhl, T. L. *Nano Lett.* **2011**, *11*, 2169–2172.
(6) Song, C. F.; Shi, W.; Jiang, H. R.; Tu, J.; Ge, D. T. *J. Membr. Sci.* **2011**, *372*, 340–345.
(7) Zhang, K. P.; Luo, Y. L.; Li, Z. Q. *Soft Matter* **2007**, *5*, 183–195.
(8) Stubenrauch, K.; Voets, I.; Fritz-Popovski, G.; Trimmel, G. *J. Polym. Sci., Part A: Polym. Chem.* **2009**, *47*, 1178–1191.
(9) Huang, J.; Hu, X. B.; Zhang, W. X.; Zhang, Y. H.; Li, G. T. *Colloid Polym. Sci.* **2008**, *286*, 113–118.
(10) Shiraki, T.; Dawn, A.; Thi, N. L. L.; Tsuchiya, Y.; Tamaru, S.; Shinkai, S. *Chem. Commun.* **2011**, *47*, 7065–7067.
(11) Hribar, K. C.; Lee, M. H.; Lee, D.; Burdick, J. A. *Acs Nano* **2011**, *5*, 2948–2956.
(12) Kim, H.; Jeong, S. M.; Park, J. W. *J. Am. Chem. Soc.* **2011**, *133*, 5206–5209.
(13) Liu, Y. J.; Liu, L. W.; Zhang, Z.; Leng, J. S. *Smart Mater. Struct.* **2009**, *18*, 095024.
(14) Lenhardt, J. M.; Black, A. L.; Craig, S. L. *J. Am. Chem. Soc.* **2009**, *131*, 10818–10819.
(15) Hussein, I. A.; Ali, S. K. A.; Suleiman, M. A.; Umar, Y. *Eur. Polym. J.* **2010**, *46*, 1063–1073.
(16) Wandera, D.; Wickramasinghe, S. R.; Husson, S. M. *J. Membr. Sci.* **2011**, *373*, 178–188.
(17) Mi, L.; Bernards, M. T.; Cheng, G.; Yu, Q. M.; Jiang, S. Y. *Biomaterials* **2010**, *31*, 2919–2925.
(18) Saitoh, T.; Mizutani, K.; Hiraide, M. *Bull. Chem. Soc. Jpn.* **2006**, *79*, 95–99.
(19) Lewis, S. R.; Datta, S.; Gui, M. H.; Coker, E. L.; Huggins, F. E.; Daunert, S.; Bachas, L.; Bhattacharyya, D. *Proc. Natl. Acad. Sci. U.S.A.* **2011**, *108*, 8577–8582.
(20) Shin, J. H.; Lee, H. L.; Cho, S. H.; Ha, J. H.; Nam, H.; Cha, G. S. *Anal. Chem.* **2004**, *76*, 4217–4222.
(21) Cheng, X. H.; Canavan, H. E.; Stein, M. J.; Hull, J. R.; Kweskin, S. J.; Wagner, M. S.; Somorjai, G. A.; Castner, D. G.; Ratner, B. D. *Langmuir* **2005**, *21*, 7833–7841.
(22) Yang, B.; Li, G. Z.; Zhang, X.; Shu, X.; Wang, A. N.; Zhu, X. Q.; Zhu, J. *Polymer* **2011**, *52*, 2537–2541.
(23) Gray, H. N.; Jorgensen, B.; McClaugherty, D. L.; Kippenberger, A. *Ind. Eng. Chem. Res.* **2001**, *40*, 3540–3546.
(24) Shim, M. S.; Kwon, Y. J. *Biomaterials* **2011**, *32*, 4009–4020.
(25) Zhang, R. S.; Tang, M. G.; Bowyer, A.; Eisenthal, R.; Hubble, J. *Biomaterials* **2005**, *26*, 4677–4683.
(26) Wang, D. Q.; Tan, J. J.; Kang, H. L.; Ma, L.; Jin, X.; Liu, R. G.; Huang, Y. *Carbohydr. Polym.* **2011**, *84*, 195–202.
(27) Li, Y. X.; Liu, R. G.; Liu, W. Y.; Kang, H. L.; Wu, M.; Huang, Y. *J. Polym. Sci., Part A: Polym. Chem.* **2008**, *46*, 6907–6915.
(28) Kang, H. L.; Liu, W. Y.; He, B. Q.; Shen, D. W.; Ma, L.; Huang, Y. *Polymer* **2006**, *47*, 7927–7934.
(29) Tan, J. J.; Kang, H. L.; Liu, R. G.; Wang, D. Q.; Jin, X.; Li, Q. M.; Huang, Y. *Polym. Chem.* **2011**, *2*, 672–678.
(30) Shen, D. W.; Yu, H.; Huang, Y. *Cellulose* **2006**, *13*, 235–244.
(31) Liu, W. Y.; Liu, R. G.; Li, Y. X.; Kang, H. L.; Shen, D.; Wu, M.; Huang, Y. *Polymer* **2009**, *50*, 211–217.
(32) Ma, L.; Kang, H. L.; Liu, R. G.; Huang, Y. *Langmuir* **2010**, *26*, 18519–18525.
(33) Ma, L.; Liu, R. G.; Tan, J. J.; Wang, D. Q.; Jin, X.; Kang, H. L.; Wu, M.; Huang, Y. *Langmuir* **2010**, *26*, 8697–8703.
(34) Ma, L.; Liu, R. G.; Wu, M.; Huang, Y. *Abstr. Pap., Am. Chem. Soc.* **2009**, *237*, 95-CELL.
(35) Yan, Q.; Yuan, J. Y.; Zhang, F. B.; Sui, X. F.; Xie, X. M.; Yin, Y. W.; Wang, S. F.; Wei, Y. *Biomacromolecules* **2009**, *10*, 2033–2042.
(36) Wan, S.; Jiang, M.; Zhang, G. Z. *Macromolecules* **2007**, *40*, 5552–5558.
(37) Tan, J. J.; Li, Y. X.; Liu, R. G.; Kang, H. L.; Wang, D. Q.; Ma, L.; Liu, W. Y.; Wu, M.; Huang, Y. *Carbohydr. Polym.* **2010**, *81*, 213–218.
(38) Takada, K.; Gopalan, P.; Ober, C. K.; Abruna, H. D. *Chem. Mater.* **2001**, *13*, 2928–2932.

(39) Merchant, S. A.; Tran, T. O.; Meredith, M. T.; Cline, T. C.; Glatzhofer, D. T.; Schmidtke, D. W. *Langmuir* **2009**, *25*, 7736–7742.
(40) Warren, S.; Doaga, R.; McCormac, T.; Dempsey, E. *Electrochim. Acta* **2008**, *53*, 4550–4556.
(41) Yang, J.; Sykora, M.; Meyer, T. J. *Inorg. Chem.* **2005**, *44*, 3396–3404.
(42) Tsujimoto, M.; Yabutani, T.; Sano, A.; Tani, Y.; Murotani, H.; Mishima, Y.; Maruyama, K.; Yasuzawa, M.; Motonaka, J. *Anal. Sci.* **2007**, *23*, 59–63.
(43) Liu, C. X.; Liu, H. M.; Yang, Q. D.; Lin, N. S.; Song, Y. L.; Wang, L.; Cai, X. X. Highly Sensitive Determination of Dopamine Using Osmium/Nafion Modified Disposable Integrated Biosensor. In *Micro and Nano Technology - 1st International Conference of Chinese Society of Micro/Nano Technology*; Wang, X., Ed.; Trans Tech Publications LTD: Stafa-Zurich, Switzerland, 2009; Vols. 60−61, pp 311−314.
(44) Havens, N.; Trihn, P.; Kim, D.; Luna, M.; Wanekaya, A. K.; Mugweru, A. *Electrochim. Acta* **2010**, *55*, 2186–2190.
(45) Torriero, A. A. J.; Salinas, E.; Battaglini, F.; Raba, J. *Anal. Chim. Acta* **2003**, *498*, 155–163.
(46) Flexer, V.; Calvo, E. J.; Bartlett, P. N. *J. Electroanal. Chem.* **2010**, *646*, 24–32.
(47) Park, T. M. *Anal. Lett.* **1999**, *32*, 287–298.
(48) Linford, R. G. *Electrochemical Science and Technology of Polymers*; Elsevier Applied Science: London/New York, 1987.
(49) Tagliazucchi, M.; Calvo, E. J.; Szleifer, I. *J. Phys. Chem. C* **2008**, *112*, 458–471.
(50) Gulyas, P. T.; Smith, T. A.; Paddon-Row, M. N. *J. Chem. Soc., Dalton Trans.* **1999**, 1325–1335.
(51) Gao, J.; Haidar, G.; Lu, X. H.; Hu, Z. B. *Macromolecules* **2001**, *34*, 2242–2247.
(52) Chauhan, G. S.; Singh, B.; Dhiman, S. K. *J. Appl. Polym. Sci.* **2004**, *91*, 2454–2464.
(53) Sidorov, S. N.; Bronstein, L. M.; Kabachii, Y. A.; Valetsky, P. M.; Soo, P. L.; Maysinger, D.; Eisenberg, A. *Langmuir* **2004**, *20*, 3543–3550.
(54) Mendrek, S.; Mendrek, A.; Adler, H. J.; Dworak, A.; Kuckling, D. *J. Polym. Sci., Part A: Polym. Chem.* **2009**, *47*, 1782–1794.
(55) Eishun Tsuchida, M. K.; Hiroyuki Nishide, M. H. *J. Phys. Chem.* **1986**, *90*, 2283–2284.
(56) Anne, A.; Demaille, C.; Moiroux, J. *J. Am. Chem. Soc.* **1999**, *121*, 10379–10388.
(57) Anne, A.; Demaille, C.; Moiroux, J. *Macromolecules* **2002**, *35*, 5578–5586.
(58) Tam, T. K.; Ornatska, M.; Pita, M.; Minko, S.; Katz, E. *J. Phys. Chem. C* **2008**, *112*, 8438–8445.